Experimental report

Surface reactivity and durability of Pt_3Co/C nanoparticles in proton-exchange membrane fuel cells (project 30-02-1025)

Location : BM30B, ERSF
18 allocated shifts
23-29 November 2011
Local contact : Vincent Ranieri

Proposer : Dr. Frédéric Maillard
Co-Proposer : Dr. Yvonne Soldo
Julien Durst
Dr Laetitia Dubau
Prof. Marian Chatenet

I. Objectives of the project

It was proposed in the project to couple electrochemical tests with XAS acquisitions on several commercial Pt_3Co/C nanoparticles (in their pristine form but also in their aged form) on which we have acquired significant experience during the last years [1-3]. We had planned to perform such measurements at the Pt L_{III} edge (11564 eV) and at the Co K edge (7709 eV) *in situ, i.e.* at various electrode potentials. The major problem we had with our newly designed cell is that the XAS signal recorded under operation (with the cell filled with the electrolyte) at the Co K edge was too small to be recorded with accuracy. This major issue has modified our initial schedule. Therefore, *in situ* experiments were recorded only at the Pt L_{III} edge, while *ex situ* experiments were recorded at both edges. In spite of this unfortunate event, we have been able to successfully conduct:

- A comparative study at both Pt L_{III} and Co K edges between the pristine commercial Pt_3Co/C catalyst (as cited above and referred hereafter as Pt_3Co/C-MDM) and two house-made catalysts with well defined structures: a Pt_3Co/C-skeleton and a Pt_3Co/C-skin.
- A comparative study at both edges between the pristine and the aged commercial Pt_3Co/C catalyst.
- An *in situ* study conducted at the Pt LIII on how the Pt_3Co/C-skeleton evolves after two different electrochemical aging procedures.

II. Determination of the pristine structure of the commercial Pt_3Co/C catalysts

It is essential to determine the structure of a pristine Pt_3Co/C cathode catalyst, to be able to discuss how it degrades upon aging in PEMFC stack. There exists numerous ways to play on the shape (distribution of the Pt and Co atoms) of a Pt_3Co nanoparticle. Starting from randomly Pt and Co atoms within a Pt_3Co nanoparticle, chemical treatments basically consist of washing the catalyst in an acidified media to leach all the cobalt atoms located at the surface of the catalyst. Acid-leaching is believed to lead to the formation of a very thin (1 or 2 atomic layers) pure platinum surface with similar structural properties than the unmodified Pt_3Co core. The obtained structure is referred to as the Pt_3Co-skeleton [4-8]. Starting from randomly Pt and Co atoms within a Pt_3Co nanoparticle, thermal treatments can also be carried out in order to (i) reduce the number of low-coordinated Pt atoms and (ii) rearrange the surface layers of the alloy catalyst in terms of structure and composition. Indeed thermal treatments yield surface segregation of the platinum atoms, at the expense of the cobalt atoms, and thus formation of a pure platinum shell. The obtained structure is referred to as the Pt_3Co-skin.

Figure III-1 presents the normalized X-ray absorption near edge structure (XANES) spectra of the three catalysts (Pt_3Co/C-MDM, -skin and –skeleton) recorded at the Pt L_3 and at the Co K edges.

No change of the oxidation state of the platinum atoms are monitored from one sample to another, in agreement with the observations of Wang *et al*. [9]. The position of the absorption edge for both catalysts is the same than for the Pt foil, E_0 = 11563 eV. The intensity of the white line is smaller for the Pt_3Co-skin than for the Pt_3Co-skeleton catalyst, indicating a reduced amount of platinum oxides in the former structure. However, both alloyed structures are very close to that of the reference Pt foil. The most interesting part is that the differences between the Pt_3Co-skin and the Pt_3Co-skeleton nanocatalysts are marked at the Co edge. Although no edge energy shift is monitored, there are great changes of the spectrum features, which can be rationalized by a change of the cobalt atomic arrangement in the nanoparticle, when comparing both Pt_3Co/C samples to the Co foil (the Co foil has an hexagonal compact structure, the Pt foil and the Pt_3Co nanoparticles a face centred cubic one), but also when comparing the Pt_3Co-skin to the Pt_3Co-skeleton.

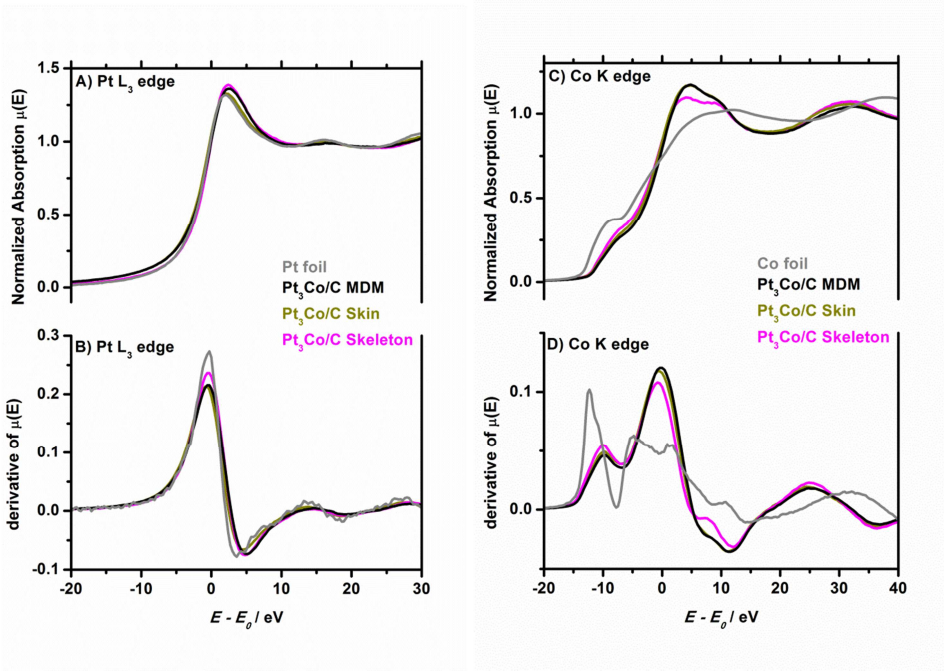

Figure III-1. XANES spectrum of the Pt_3Co/C MDM (in black), the Pt_3Co/C skeleton (in khaki) and the Pt_3Co/C skin (magenta) catalysts recorded at the (A) Pt L_3 and (B) Co K edges. The 0 on the X-axis corresponds to the absorption edge energy of the respective absorbing element E_0. The spectra recorded with Pt and Co foils are shown for comparison (in grey). The derivatives of the XANES spectra are shown in B and D for the Pt L_3 and Co K edges, respectively.

Figure III-2 displays the k^2 weighted EXAFS spectra recorded at the Pt L_3 (Figure III-2A) and at the Co K (Figure III-2B) edges. The corresponding Fourier transforms (FT) of the k^2-weighted EXAFS oscillations are shown in Figure III-3. For the Pt_3Co/C-skeleton, the values of the average first shell coordination number for a platinum atom and cobalt atom are very close: N_{Pt} = 9.5 ± 1.0 *vs.* N_{Co} = 9.5 ± 0.9. Those numbers are less than the expected value of 12 for a bulk face centred cubic structure but can easily be rationalized by considering the nanometric dimension of the catalysts (high

surface to bulk atom ratio for a 4 nm particle). The fact that similar values N_{Pt} and N_{Co} are found indicates that the platinum and the cobalt atoms are randomly and homogeneously distributed within the Pt_3Co/C-skeleton structure.

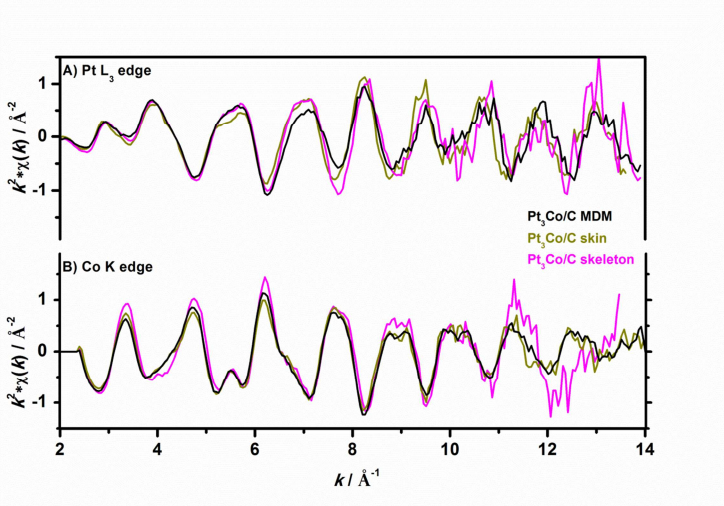

Figure III-2. k^2 weighted EXAFS spectra of the Pt_3Co/C MDM (in black), the Pt_3Co/C skeleton (in purple) and the Pt_3Co/C skin (in khaki) catalysts recorded ex situ at the (A) Pt L_3 and (B) Co K edges.

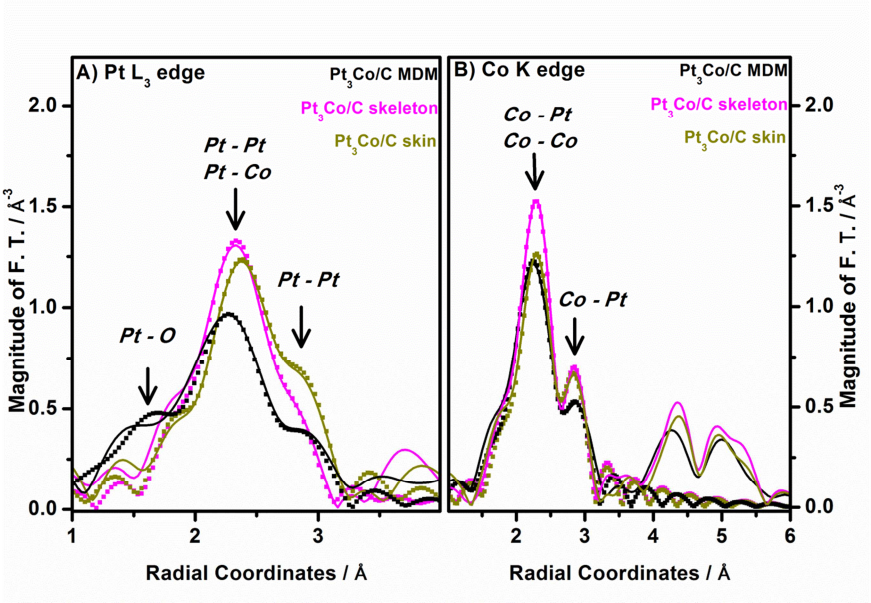

Figure III-3. Fourier Transform magnitudes of $k^2\chi$ (k) EXAFS spectra at (A) the Pt L_3 and (B) the Co K edges for the Pt_3Co/C MDM (in black), the Pt_3Co/C-skeleton (in purple) and the Pt_3Co/C-skin (in khaki) catalysts. The full lines are the experimental data and the dotted lines are the fitted data.

The results obtained for the Pt_3Co/C-skin catalyst differ slightly. The average first shell coordination numbers differ, whether the Pt or Co atomic environment is considered: N_{Pt} = 11.1 ± 1.1 and N_{Co} = 7.4 ± 0.7. According to Greco *et al.* [13], modifications of the cobalt atoms coordination

number (whereas platinum remains unaffected by the thermal treatment) can be accounted for by considering that the EXAFS signals for the Co atoms are extremely sensitive to substitutional disorder, so their intensities can be used as a measurement of the ordering level. Interestingly, the Debye-Waller values also indicate that the Co local structure is more disordered (larger Debye-Waller values) than the Pt local structure (smaller Debye-Waller values), which may confirm the hypothesis of Greco *et al.* [13]. In this frame, the smaller cobalt average coordination number observed might sign different structures adopted by the Pt_3Co/C-skin catalyst.

The first-shell interatomic distances estimated from the analyses of EXAFS spectra (Pt-Pt, Pt-Co and Co-Pt but not Co-Co) are found to be less contracted by 1 % in the skin than in the skeleton structure. The fact that the Co-Co bond length remains unaffected by the thermal treatment in the skin catalyst may be an indirect proof that the Co atoms are located in the core of the nanoparticle after the heat treatment (the Co rich core would remain unaffected by the relaxed Pt rich skin surface).

Interestingly, the structural parameters derived from the analysis of the EXAFS signals on the Pt_3Co/C MDM are essentially similar to those found on the Pt_3Co/C-skin catalyst., and confirm the results obtained on the XANES. From the reasoning on the average coordination number and the relaxed Pt-Pt bond length, we are able to conclude on a core/shell structure for the Pt_3Co/C MDM catalyst, similar to that of the Pt_3Co/C-skin.

III. Pristine vs. aged Pt_3Co/C catalysts structures

To get insights into the fine nanostructure of the aged Pt_3Co/C cathode catalysts, these were also investigated by XAS. Figure III-4 and Figure III-5 show the k^2-weighted EXAFS and the Fourier transforms of the k^2-weighted EXAFS oscillations recorded on the fresh Pt_3Co/C MDM and on two aged catalysts (the catalyst after t = 1124 h of ageing at I = 50 A, which was found to be partially depleted in cobalt but kept a homogeneous distribution of the atoms, and the catalyst aged during t = 1341 h at I = 20 A, for which compact, depleted in Co and spherically shaped “hollow” nanoparticles were found. Both aged Pt-Co/C catalysts feature an increase of the Pt and Co average coordination numbers with respect to the fresh catalyst. The rationale for that is believed to be the increase of the mean particle size observed for the aged catalysts. Indeed, the average coordination numbers determined at the Pt L_{III} edge for the aged Pt-Co/C catalysts are close to those predicted for a 7 nm cuboctahedral f.c.c nanoparticle (calculated average coordination number of $N_{A\text{-}B} \approx 11$) or for a bulk f.c.c. crystal ($N_{A\text{-}B} = 12$). Two results extracted at the Co edge are interesting to point out: (i) similar to what was observed for the fresh Pt-Co/C catalyst, the number of Co closest neighbours is much smaller than that of Pt atoms, suggesting that, when cobalt is still present in the particles, it remains

confined in the core of the catalyst during the aging process within the same particular structure (presence of vacancies) and (ii) the number of Co-Co neighbours significantly decreases at the benefit of Co-Pt neighbours. The latter confirms quantitatively that cobalt atoms have been leached out from the catalyst structure during the aging process. Interestingly, the interatomic distances found on the aged catalysts are very similar to the fresh Pt_3Co/C catalyst, even though an increase of the interatomic distances on the aged catalysts might have been expected from XRD measurements.

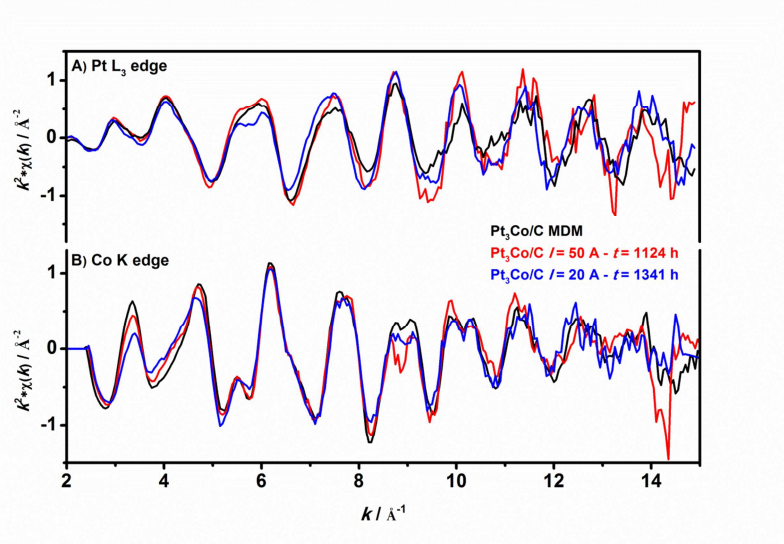

Figure III-4. k^2 weighted EXAFS spectra of the fresh Pt_3Co/C MDM (in black) and the aged catalysts having either homogeneous particles (in red, aged at I = 50 A for t = 1124h) or core-shell/hollow particles (in blue, aged at I = 20 A for t = 1341h) recorded ex situ at the (A) Pt L_3 and (B) Co K edges.

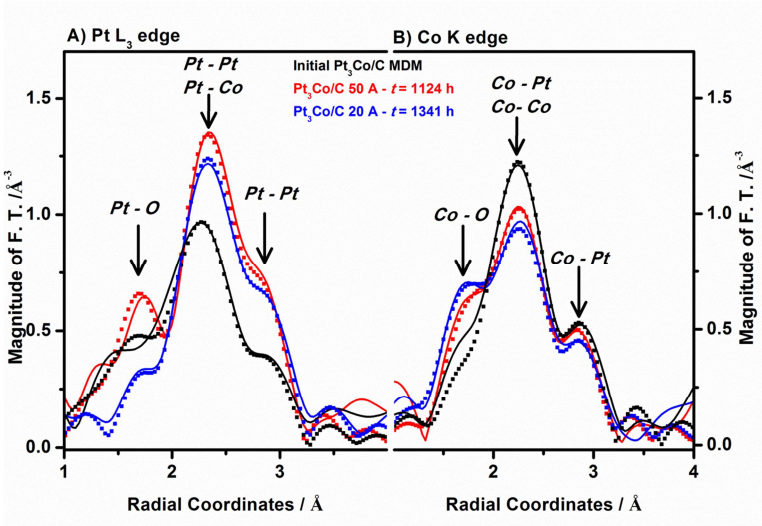

Figure III-5. Fourier transform magnitudes of the fresh Pt_3Co/C MDM (in black) and the aged catalysts having either homogeneous distribution of Pt and Co atom (in red, aged at I = 50 A for t = 1124h) or hollow particles (in blue, aged at I = 20 A for t = 1341h) recorded ex situ at the (A) Pt L_3 and (B) Co K edges. The full lines are the experimental data and dotted lines are the fitted data.

One can also notice that the fits of the EXAFS signals on the aged catalysts greatly improve when Co-O bonds are implemented (see plain and dashed lines in Figure III-5). Actually, fitting reasonably the EXAFS signals at the Co edge without an interaction of the cobalt with a lighter atom such as oxygen (carbon or fluorine would have also fit, but are less likely) would not have been possible. It can be interpreted as the presence of Co-O bonds underlying the Pt surface atoms or oxidized Co atoms located in the ionomer of the cathode catalyst layer. For pH ≥ 5, the formation of cobalt oxides is thermodynamically possible [14]. Another explanation for the formation of cobalt – oxide bonds might be that the mechanism of subsurface cobalt corrosion involves oxygen adsorption/absorption.

IV. Accelerated aging tests: How the instability of the non-noble metal content is put forth

In what follows, we present *in situ* XAS measurements aimed at showing how the fine nanostructure of a Pt_3Co/C catalyst changes during accelerated electrochemical degradation tests. In the first aging procedure (*Aging #1*) the electrode potential was linearly swept between E = 0.25 V and E = 0.85 V *vs.* RHE at v = 0.002 V s^{-1}. This aging cycle was repeated 70 times (total duration of the experiment ≈ 11 h 30 min). In the second aging procedure (*Aging #2*), potential steps at *ca.* E = 0.25 V and E = 0.85 V *vs.* RHE were successively applied for t = 10 s each. This aging cycle was repeated 140 times (total duration of the experiment ≈ 4 h). The electrode potential was maintained at E = 0.7 V *vs.* RHE during the acquisition of XAS spectra, Final XAS acquisitions performed at the end of each of the aging procedures were recorded at E = 0.25 V (non-oxidizing conditions), 0.7 V (mild oxidizing conditions) and 0.85 V (oxidizing conditions) *vs.* RHE.

Figure IV-1A displays the k^2 weighted EXAFS spectra recorded on the Pt_3Co/C-skeleton catalyst at the beginning (in black) and the end of the aging test (aging #1 in red and aging #2 in green). The corresponding Fourier Transform magnitudes of $k^2\chi$ (k) EXAFS spectra are presented in Figure IV-1B. The fitted data show minor structural changes during the accelerated aging procedure. In particular, no variation of the XANES spectra or of the characteristic atom bond length was detected during the accelerated ageing procedure. However, the latter is not surprising since the XANES spectra recorded at the Pt L_{III} edge and the characteristic atom bond lengths of the catalyst were not shown to be impacted for MEAs aged for more than 1000 hours in real PEMFC conditions (see the previous paragraph). *Aging #1* has caused the decrease of the number of cobalt neighbours at the expense of an increase of the number of platinum neighbours. After *Aging #2,* there is an overall decrease of the total coordination number, which would translate into a slight decrease of the mean particle size. This can be easily rationalized as follows: the accelerated aging procedure is thought to exacerbate the rapid dissolution of low-coordinated surface atoms, yielding dissolution of the smallest

particles. In PEMFC operating conditions, the released Pt^{z+} ions possess sufficiently long residence time in the MEA to redeposit onto larger particles leading to the increase of the mean particle size. However the coupled XAS-electrochemical cell used in this study operates under constant liquid circulation, which facilitates removal of Pt^{z+} and Co^{2+} ions out of the catalyst layer.

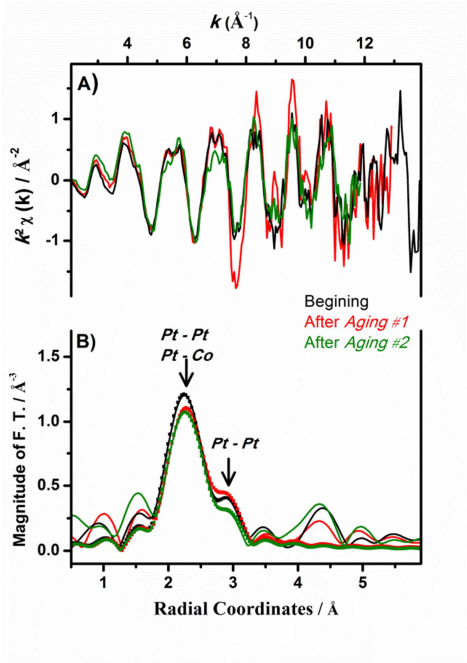

Figure IV-1. (A) EXAFS spectrum k^2 weighted and (B) Fourier transform magnitudes of $k^2\chi$ (k) EXAFS spectra recorded at the Pt L_3 edge at an applied potential E = 0.70 V vs. RHE on the fresh Pt_3Co/C catalyst (in black) and on the aged Pt_3Co/C catalyst (after Aging #1 in red and after Aging #2 in green). The full lines are the experimental data and the dotted lines are the fitted data.

V. Conclusion

In the frame of this project, we have been able to:

- Unveil a core/shell structure for the pristine commercial Pt_3Co/C MDM catalyst, similar to that of the Pt_3Co/C-skin catalyst.
- Confirm that this type of Pt_3Co/C catalyst undergo strong modifications of its pristine structure after being aged in a PEMFC,
- And confirm *in situ* that accelerated electrochemical aging tests, which are now widely used to assess the stability of Pt_3Co/C catalyst materials in acidic medium, fail to reproduce their degradations that occur in a PEMFC system.

Clearly, it would have been interesting to study the effect of a long-term durability test, with larger number of potential modulations that in this study. However, the high Pt-Co/C loadings required for XAS measurements, which cause facile gas evolution (ohmic drop) when using large potential scan rates, did prevent further measurements over a greater duration. It is also important to note that the limited beam time at ESRF (18 shifts) is not compatible with long-term *in-situ* aging tests. It would also have been interesting to work *in situ* at the Co K edge, as we have seen that in the case of aged Pt_3Co/C nanoparticles, most of the structural changes that have occurred are observed mostly at the Co K edge. By enhancing the concentration in cobalt and by modifying the cell to reduce the amount of electrolyte in it, this should be fixed for the next set of XAS measurements.

These results have been published in the thesis report of Julien Durst [15]. As they are believed to be of high relevance, they will also be published in a peer-reviewed journal as soon as possible.

VI. References

[1] F. Maillard, L. Dubau, J. Durst, M. Chatenet, J. André, E. Rossinot, Electrochem. Commun., 12 (2010) 1161-1164.
[2] L. Dubau, J. Durst, F. Maillard, L. Guétaz, M. Chatenet, J. André, E. Rossinot, Electrochim. Acta, 56 (2011) 10658-10667.
[3] L. Dubau, J. Durst, F. Maillard, M. Chatenet, J. André, E. Rossinot, Fuel Cells, 12 (2012) 188-198.
[4] T. Toda, H. Igarashi, H. Uchida, M. Watanabe, J. Electrochem. Soc., 146 (1999) 3750-3756.
[5] I.E.L. Stephens, A.S. Bondarenko, L. Bech, I. Chorkendorff, Chem. Cat. Chem, 4 (2012) 341-349.
[6] P. Strasser, S. Koh, T. Anniyev, J. Greeley, K. More, C. Yu, Z. Liu, S. Kaya, D. Nordlund, H. Ogasawara, M.F. Toney, A. Nilsson, Nat. Chem., 2 (2010) 454-460.
[7] S. Chen, W.C. Sheng, N. Yabuuchi, P.J. Ferreira, L.F. Allard, Y. Shao-Horn, J. Phys. Chem. C, 113 (2009) 1109-1125.
[8] V.R. Stamenkovic, B.S. Mun, K.J.J. Mayrhofer, P.N. Ross, N.M. Markovic, J. Am. Chem. Soc., 128 (2006) 8813-8819.
[9] C. Wang, M. Chi, D. Li, D. Strmcnik, D. van der Vliett, G. Wang, V. Komanicky, K.-C. Chang, A.P. Paulikas, D. Tripkovic, J. Pearson, K.L. More, N.M. Markovic, V.R. Stamenkovic, J. Am. Chem. Soc., 133 (2011) 14396-14403.
[10] F.J. Lai, L.S. Sarma, H.L. Chou, D.G. Liu, C.A. Hsieh, J.F. Lee, B.J. Hwang, J. Phys. Chem. C, 113 (2009) 12674-12681.
[11] F.J. Lai, W.N. Su, L.S. Sarma, D.G. Liu, C.A. Hsieh, J.F. Lee, B.J. Hwang, Chem.-Eur. J., 16 (2010) 4602-4611.
[12] D.S. Kim, J.H. Kim, I.K. Jeong, J.K. Choi, Y.T. Kim, J. Catal., 290 (2012) 65 - 78.
[13] G. Greco, A. Witkowska, E. Principi, M. Minicucci, A. Di Cicco, Phys. Rev. B, 83 (2011).
[14] A. Greszler, T. Moylan, H.A. Gasteiger, Modeling the impact of cation contamination in a polymer electrolyte membrane fuel cell, in: W. Vielstich, H.A. Gasteiger, H. Yokokawa (Eds.) Handbook of Fuel Cells: Fundamentals, Technology, and Applications, vol. 4, John Wiley & Sons, Chichester, 2009.
[15] J. Durst, Etude du Vieillissement des Assemblages Membrane-Electrodes pour Piles à Combustible Basse Température, in: Grenoble INP, Grenoble, Grenoble, 2012.